# Dynamical Symmetry Analysis of Ionization and Harmonic Generation of Atoms in Bichromatic Laser Pulses

**AVNER FLEISCHER,[1] ASHISH KUMAR GUPTA,[1,2] NIMROD MOISEYEV[1]**

[1]*Department of Chemistry and Minerva Center for Nonlinear Physics of Complex Systems, Technion–Israel Institute of Technology, Haifa 32000, Israel*

[2]*Department of Chemistry, Indian Institute of Technology, Guwahati, North Guwahati, Guwahati 781039, India*

*Received 1 December 2004; accepted 13 December 2004*
*Published online 22 March 2005 in Wiley InterScience (www.interscience.wiley.com).*
*DOI 10.1002/qua.20541*

**ABSTRACT:** Recently the effect of the relative phase $\phi$ in a high-intensity ($\sim 10^{14}$ W/cm$^2$) two-color (bichromatic) CW laser with frequencies $\omega$ and $2\omega$ on the high-order harmonic generation (HHG) was studied within the framework of the non-Hermitian quantum mechanics (NHQM) [Phys Rev A 2004, 69, 043404/1]. Here we emphasize the study of symmetries in bichromatic HHG spectra within the framework of the conventional Hermitian QM, and in particular by taking the duration of the laser pulse into consideration (an effect that has not been included in the non-Hermitian studies due to the time asymmetry problem in NHQM). The phase dependence of HHG and intense-field ionization probability in a 1D Xe atom with symmetric field-free potential and symmetric initial wave function were studied numerically and analytically. From simulations based on a single-particle response it can be seen that the HHG spectra is symmetric with respect to inversion in the relative phase between the two colors $\phi$ only if ionization is forbidden in the system and the laser pulse is an adiabatic one. The HHG spectra is symmetric with respect to a $\pi$-shift in $\phi$ whenever the laser pulse is an adiabatic one, either for bound or open (ionized) systems. The ionization probability is symmetric both to inversion or $\pi$-shift in $\phi$; the component probabilities (right- and left-ionization probabilities) have the same $\phi$-dependence, up to a shift of $\pi$.  Int J Quantum Chem 103: 824–840, 2005

**Key words:** photo-induced ionization; high order harmonics; atoms in bichromatic strong laser pulses; nonlinear phenomenon

*Correspondence to:* N. Moiseyev; e-mail: nimrod@techunix.technion.ac.il

## 1. Introduction

HHG is a nonperturbative phenomenon in which a target system (gaseous sample of atoms/ions/molecules, atomic clusters, solid target) interacts with an intense laser field and as a result emits high-order harmonics of the incident laser frequency [2, 3]. The phenomena owes its existence to the highly nonlinear response of the time-dependent induced electric dipole moment to the external laser field. Among the limited number of methods that do exist [1], HHG stands as one of the most promising methods of producing short fs pulses of coherent radiation in the extreme ultraviolet (XUV) range. However, the major problem of the HHG phenomenon is its low conversion efficiency (the flux of emitted high harmonics is usually much smaller than the incident radiation flux). This problem need to be solved before coherent X-ray sources based on HHG can be built.

The process of HHG can be understood from both a semiclassical and a quantum-mechanical point of view in terms of the interaction of a single electron with its nucleus and the external driving force [this approximation is called a single atom response (SAR) approximation]. According to the semiclassical interpretation, in the low-frequency–high-intensity regime (Keldysh parameter $\leq 1$) HHG is a three-step process. In the first step the initially bounded electron tunnels or multiphoton ionizes into the continuum (through the potential barrier formed by the combined atomic and electromagnetic field) with some initial velocity. The electron then accelerates back and forth along the field, as a free particle, and gains a kinetic energy that depends on the field parameters and on the time the electron was "born" (the time it appeared in the continuum). If the electron returns to the vicinity of the parent ion it may recombine to the ground state, thus emitting high-energy photons with energy equal to the sum of the ionization potential and the kinetic energy of the electron gained in the field. Because this kinetic energy has a maximal possible value, there is an approximate value of the highest harmonic that can be obtained. According to the quantum mechanical picture the electron is represented as a wavepacket that propagates under the influence of the field; it oscillates back and forth and also partially spreads over the continuum. These oscillations of the electron near the nucleus cause the formation of radiation.

The typical HHG emission spectra of atomic system in the low-frequency–high-intensity regime exhibit three parts: an initial decreasing part, a plateau, which can be considered as a signature of the nonlinearity of the process, and eventually a further sharply decreasing part. The approximate value of the highest harmonic in the plateau is called the "cut-off" position and, according to the above semiclassical picture, corresponds to the maximum kinetic energy of the electron upon return to the nucleus.

Many experimental and theoretical studies have been carried out to search for ways to enhance HHG production and extend the spectrum of the emitted harmonics to higher frequencies. Most studies in the last decade have been concerned with generation of odd harmonics by focusing intense short laser pulses of linear polarization and a single frequency into a jet of rare-gas atoms [4]. Other studies deal with systems possessing special symmetry properties, which introduce selectivity and/or enhancement in the generation of high harmonics [5]. Such systems include, for example, the benzene molecules [6], thin graphite sheets [7], or carbon nanotubes [8] interacting with circularly polarized radiation. The influence of the laser parameters (such as intensity, polarization, wavelength, pulse shape, and duration) on the HHG spectra has been studied extensively as well.

The use of a two-color (bichromatic) laser beam with frequencies $\omega$ and $2\omega$ and relative phase $\phi$ [Eq. (6)] in HHG experiments has been shown to greatly modify the HHG power spectra. In addition to the regular odd harmonics that appear in a one-color HHG experiment, even harmonics now also appear. The conversion efficiency of high harmonics is enhanced by up to two orders of magnitude, when compared with one-color laser experiments (extended plateau). By adjusting the relative intensities, relative frequencies, polarizations, and the relative phase between the driving fields, it is possible to enhance or suppress groups of harmonics. The shape and maximum amplitude of the time-varying field is a strong function of $\phi$ (while the average intensity remains the same), as is shown in Figure 1. Changing the value of $\phi$ alters the instantaneous field amplitude (the amplitude of the field when the electron is "born") and hence is an effective way of controlling the HHG process, since this amplitude determines the initial conditions of the process and hence the kinetic energy acquired by the electron.

Because HHG is a nonlinear process, the harmonic strength is not a trivial function of $\phi$ and, in

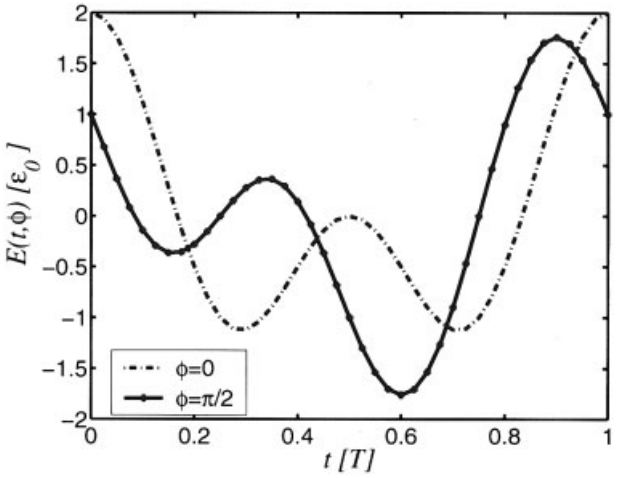


**FIGURE 1.** The electric field given in Eq. (6) for $\phi = 0$ and $\phi = \pi/2$.

addition, different harmonics depend differently on $\phi$. Since there has been some debate in the literature regarding the dependence of the spectrum on $\phi$ and especially regarding the symmetries that the HHG spectra possess [9–12], we wish to investigate the existence of symmetries that involve $\phi$, under which the HHG spectrum is invariant. We will show that, under the model used here, the only relevant symmetries are the inversion and/or the translation of $\phi$ by $\pi$. The quality of experimental data provided by Andiel et al. [13] does not allow us to reach conclusions regarding the symmetries that do exist (propagation effects tend to average out the highly sensitive SAR). Other theoretical and experimental sources give different results (compare Refs. [9] and [10] with [11]). This question therefore should be investigated carefully and thoroughly. The existence of symmetries in the HHG spectra could be found through pure theoretical analysis of the problem, which is called dynamical symmetry analysis (DSA). However, unless DSA states that symmetry exists in the problem, it cannot reveal the exact extent of asymmetry for problem where the symmetry does not exist. Numerical simulations still need to be performed to calculate the exact extent of asymmetry. Nevertheless, the preliminary information provided by DSA is important as it can hint which symmetries exist in the problem, which parameters (physical conditions) have influence on these symmetries, and therefore in which type of numerical simulations/real experiments these symmetries will be present.

For CW lasers, within the framework of the conventional Hermitian QM, the HHG spectrum calculated using a single Floquet state, or any finite number of Floquet states, is invariant under the inversion of the relative phase of the two frequency components, $\phi \rightarrow -\phi$ [14]. The asymmetry with respect to the phase inversion seen in the simulated HHG spectra is obtained in the conventional QM *only* when the Floquet spectrum is continuous and ionization is taken into consideration. Because of the time-asymmetric problem in non-Hermitian QM (NHQM), we could not perform motion of wave-packet calculation when the time is taken from 0 to $-\infty$ and calculate the time-dependent dipole moment. We have avoided this difficulty by calculating the HHG spectra for CW lasers, using the complex-scaled Floquet theory (and not the Hermitian) [14]. For CW lasers we found that there is a direct correlation between the strength of the asymmetry with respect to the relative phase inversion and the magnitude of the ionization rate. How can this relationship between photo-induced ionization and symmetry properties of the HHG spectra be explored within the conventional Hermitian QM? What is the effect of the duration of the laser pulse on that relationship? What is the effect of the relative phase in a two-color field on the photo-induced ionization and on its correlation with the HHG spectra? The answers to these questions, which may simulate further experiments in this field, were the aim of our research, the results of which we present in this article. Note that the last subject is, in a way, a complementary study to the theoretical and experimental studies by Baltuska [15], Krausz's group [16], and Bandrauk et al. [17] on the carrier-envelope relative phase effect on the ionization asymmetry when short laser pulses are applied.

Here we show that the two parameters that influence the existence of the symmetries are the duration of the laser pulse (i.e., the adiabaticity property) and the existence of ionization (i.e., ionization rate). To explore this, we carried out numerical calculations for two different cases, one of them being nonphysical since the spectrum was discrete (two-level system).

We should clarify that in the following sections the expressions we derived are applicable for any high-order harmonics. For illustration, we show the results obtained for the third harmonic. Note, however, that very similar results were obtained for all other high-order harmonics.

## 2. Simulating HHG on a Xe Atom

To determine the existence of symmetries in the HHG emission spectra, we first need to introduce the Hamiltonian of the problem. We chose to investigate a single active electron 1D Hamiltonian (in the $x$-axis), which simulates the outer electron of an isolated Xe atom in an intense laser field.[1] The electron is driven by a bichromatic laser field that is intense enough to be treated classically (in the sense that its intensity is not expected to change as a result of the interaction with the atom). The laser field is linearly polarized along the $x$-axis where the laser beam propagates in the $z$-direction.[2] The evolution of the atomic system embedded in the radiation field is described by the following time-dependent Schrödinger equation (TDSE) written in the length gauge:

$$H(x, t; \phi)\Psi(x, t; \phi) = i\hbar \frac{\partial}{\partial t}\Psi(x, t; \phi), \quad (1)$$

where the time-dependent Hamiltonian is

$$H(x, t; \phi) = -\frac{\hbar^2}{2m}\frac{\partial^2}{\partial x^2} + V(x, t; \phi), \quad (2)$$

where

$$V(x, t; \phi) = V_0(x) - d(x) \cdot f(t) \cdot E(t, \phi), \quad (3)$$

and the wave function was taken initially at the symmetric ground state (g.s.) of the field-free Hamiltonian of the system:

$$\Psi(x, t = 0; \phi) = \varphi_0(x) \quad \vee \phi. \quad (4)$$

The field-free effective potential $V_0(x)$ is an inverse Gaussian

$$V_0(x) = -0.63 \exp(-0.1424x^2), \quad (5)$$

which supports two bound states that mimic the two lowest electronic states of Xe, with energies $E_0 = -0.4451$ au, $E_1 = -0.1400$ au and a third weakly bound state with energy $E_2 = -0.00014$ au (see Fig. 2).

$E(t, \phi)$ is the electric field generated by the bichromatic laser beam of frequencies $\omega$ and $2\omega$ and relative phase $\phi$ where $\varepsilon_1$, $\varepsilon_2$ represents the maximum amplitude of the single colors and were taken here to be the same value $\varepsilon_1 = \varepsilon_2 \equiv \varepsilon_0$:

$$E(t, \phi) = \varepsilon_1 \cos(\omega t) + \varepsilon_2 \cos(2\omega t + \phi) = \varepsilon_0[\cos(\omega t) + \cos(2\omega t + \phi)]. \quad (6)$$

$d(x) = ex$ is the dipole moment of the system with $e$ as the electron charge; the function $f(t)$ represents the pulse shape (laser envelope). Depending on which laser envelope is taken, the Hamiltonians needs to be solved is (in atomic units: $\hbar = m = 1$, $e = -1$)

$$H(x, t; \phi) = -\frac{1}{2}\frac{\partial^2}{\partial x^2} - 0.63 \exp(-0.1424x^2) + xf(t)\varepsilon_0[\cos(\omega t) + \cos(2\omega t + \phi)]. \quad (7)$$

For reasons that will become clear soon, we decided to explore two cases: in the first, the envelope of the incident radiation is in the form of a symmetric sine-square pulse and, in the second case, the envelope simulates an adiabatically switched "$1 - \exp(-at^2)$"-pulse (the case for CW laser was studied

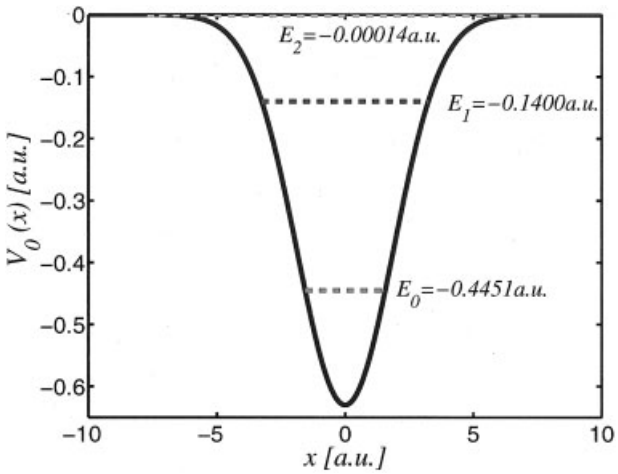


**FIGURE 2.** The field-free potential used to simulate the 1D Xe atom.

[1]Macroscopic collective effects due to propagation of the scattered light in a medium or the superposition of radiation emitted by different atoms are therefore all excluded.

[2]To reduce numerical efforts in multidimensional problems, it is usually assumed that the laser wavelength is large enough so that the electron does not feel any spatial gradient of the field during its excursion around the nucleus. This so-called "dipole approximation," in which only the temporal dependence of the field is kept, exists inherently in any 1D model and also in our model.

in Ref. [14]). The function $f(t)$, which represents the laser envelope, has the following form:

$$f(t) = \sin^2\left(\frac{\omega t}{2N}\right) o \le t \le NT \text{ or } f(t) = 1 - \exp(-at^2; t > 0) \quad (8)$$

where $N$ is the number of time periods $T$ ($T = 2\pi/\omega$) that enter the pulse and $a$ is a small-enough parameter.

During all simulations the parameters $\varepsilon_0 = 0.035$[3] and $\omega = 0.0924$ ($\lambda = 493$ nm) were used.

According to the laws of classical electrodynamics, within the dipole approximation, an accelerating particle emits radiation isotropically with time-dependent intensity proportional to the square of the second time derivative of its position, i.e., to the square of its time-dependent acceleration (Larmor's formula, see Ref. [18]):

$$I_{\text{classical}}(t) = \frac{2e^2}{3c^2}\left|\frac{\partial^2}{\partial t^2}\vec{r}(t)\right|^2. \quad (9)$$

For systems behaving according to the laws of quantum mechanics (QM), the QM analogue of the acceleration must be used. Following the classical-quantum correspondence principle, this is the time-dependent dipole acceleration expectation value (which is the second derivative of the time-dependent-induced electric dipole moment, but can be computed by means of Ehrenfest's theorem as well, as the expectation value of minus the gradient of the time-dependent potential):

$$\begin{aligned} a(t;\phi) &\equiv e^{-1}(t;\phi) \\ &= e^{-1}\frac{\partial^2}{\partial t^2}\langle\Psi(x,t;\phi)|x|\Psi(x,t;\phi)\rangle \\ &= m^{-1}\left\langle\Psi(x,t;\phi)\right| -\frac{\partial V(x,t;\phi)}{\partial x}\left|\Psi(x,t;\phi)\right\rangle \\ &= m^{-1}\left\langle\Psi(x,t;\phi)\right| -\frac{\partial V_0(x)}{\partial x} \\ &\quad + e\cdot f(t)\cdot E(t,\phi)\left|\Psi(x,t;\phi)\right\rangle. \end{aligned} \quad (10)$$

The spectral resolution of the intensity, what we would call the HHG *power spectra* $\sigma(\Omega)$ of the emitted radiation (the rate of emission of radiation in frequency $\hbar\Omega$, which may be a multiple of $\hbar\omega$ but does not have to be), is obtained from Eq. (9) where the modulus of the Fourier transform of the time-dependent acceleration is squared and the constant coefficient need to be taken twice as big (the $\Omega$ and $-\Omega$ components of the emitted radiation are indistinguishable[4]). Finally,

$$\sigma(\Omega;\phi) \propto \left|\frac{1}{T_p}\int_0^{T_p} a(t;\phi)e^{-i\Omega t}dt\right|^2, \quad (11)$$

where $T_p = NT$ is the length of the laser pulse. We are interested in the power spectra only at integer harmonic frequencies (and not in side bands) $\sigma(\Omega = n\hbar\omega;\phi)$, where $n$ is an integer. The reason is that, for these, our theoretical results could be easily reproduced in the lab (integer harmonics are phase matched in a medium and therefore propagate with a minimal loss).

As explained in the following section, DSA hints that under the conditions presented, (only) two symmetries have the potential to appear in the spectra of a certain harmonic $n$:

$$\sigma(\Omega;\phi) = \sigma(\Omega;-\phi) \quad \text{(I)}$$

$$\sigma(\Omega;\phi) = \sigma(\Omega;\phi+\pi). \quad \text{(II)}$$

Let us define the following asymmetry parameters, which measure quantitatively the extent to which the relations (I) and (II) hold:

$$\Delta\sigma_{\text{I}}(\Omega) \equiv \frac{\int_0^{\pi}|\sigma(\Omega;\phi)-\sigma(\Omega;-\phi)|d\phi}{\int_0^{\pi}\sigma(\Omega;\phi)d\phi} \quad \text{(Ia)}$$

[3]For monochromatic field, the intensity $I_0$ is proportional to the square of the maximum amplitude of the field: $I_0 = (c/8\pi)\varepsilon_0^2$. For bichromatic field, the average intensity equals $(c/8\pi)(\varepsilon_1^2 + \varepsilon_2^2)$ but the peak intensity $I_{\text{peak}} = (c/8\pi)[\max(|E(t,\phi)|)]^2$ is $\phi$-dependent. A value of $\varepsilon_0 = 0.035$ corresponds to an intensity of $I_0 = 4.3\cdot10^{13}$ W/cm$^2$ in the monochromatic case, $I_0 = 8.6\cdot10^{13}$ W/cm$^2$ in the bichromatic case and peak intensity which may range between $1.3\cdot10^{14}$ W/cm$^2$ and $1.7\cdot10^{14}$ W/cm$^2$, since the two extreme values for the maximum amplitude of the field are $\max(|E(t,\phi)|) \cong 1.76$ (obtained, for example, for $\phi = \pi/2$) and $\max(|E(t,\phi)|) \cong 2$ (obtained, for example, for $\phi = 0$).

[4]For any real function $f(x)$ the power spectra is symmetric since $f(x) = f^*(x) \to \bar{f}(k) = \bar{f}^*(-k)$ ($\bar{f}(k) \equiv (1/\sqrt{2\pi})\int_{-\infty}^{\infty} f(x)e^{-ikx}dx$) so by multiplying the former equality by its complex conjugate we get $|\bar{f}(k)|^2 = |\bar{f}(-k)|^2$.

$$\Delta\sigma_{\mathrm{II}}(\Omega) \equiv \frac{\int_0^{\pi} |\sigma(\Omega;\phi) - \sigma(\Omega;\phi+\pi)| d\phi}{\int_0^{\pi} \sigma(\Omega;\phi) d\phi}, \qquad \text{(IIa)}$$

when (I) holds $\Delta\sigma_{\mathrm{I}}(\Omega) \to 0$, etc.

Once more, DSA considerations are used, this time to check which parameters have the potential to influence the values of the asymmetry parameters. It will become evident that the existence of *ionization* in the system[5] and the length of the laser pulse[6] are the two main parameters that influence the existence of symmetries (I) or (II) in the HHG emission spectra and should be checked thoroughly. Therefore, the preliminary results obtained from simple DSA help us design the Hamiltonian of the problem and two simulations to check the existence of the symmetries in which the atom is submitted to a sine-square laser pulse, with ionization forbidden or allowed. The numerical methods used to solve the TDSE with the laser pulse were the split operator Forest–Ruth algorithm [19, 20] with 7 points and the sixth-order Runga–Kutta–Verner algorithm ([21]); the grid size, time step, and/or grid step were adjusted as required to achieve convergence.

[5]Ionization is a relevant physical quantity in the context of HHG because it acts as an inhibitor: when the atom is totally ionized, the dipole does not radiate anymore. To allow ionization in simulations, one needs to take a system that has localized bound states as well as unlocalized continuum states. As the initial bound localized wave function propagates under the influence of the field, some portion of it is released into the (unlocalized) continuum and hence not all of the population remains in the bound states at the end of the pulse.

[6]The shape of the laser, the shape of the field-free potential, and the shape of the initial condition wave function are parameters that have influence as well. But these parameters were taken as symmetric functions (sine-square, Gaussians), in order to "assist," as much as possible, the appearance of the two symmetries. In this sense DSA not only hints which symmetries may appear in the problem and what parameters influence their existence, but also hints what Hamiltonian (which physical conditions) should be taken in order to aid the appearance of the two symmetries.

## 3. DSA of General Time-Dependent Problems

Dynamical symmetries (DSs) are the symmetries of the equations of motion, in our case the TDSE. They are, in general, time-dependent transformations that, upon action on the TDSE, transform its solution into another solution, which satisfies the same equation [22].

DSA developed in Ref. [8] was for time periodic fields or for a time-periodic series of infinite number of laser pulses. That DSA was carried out for the eigenfunctions of the Floquet operator. Here we carry out the DSA for the solutions of the time-dependent Schrödinger equation. Our approach also holds for wave-packet simulation calculations.

In our case, the DSs of the system could be determined directly from the Hamiltonian, because its structure is simple.[7] Let $\hat{P}$ be a transformation that leaves both the Hamiltonian and the operator $i\hbar(\partial/\partial t)$ invariant under its action:

$$\hat{P}\hat{H}\hat{P}^{-1} = \hat{H};\ \hat{P}\left(i\hbar\frac{\partial}{\partial t}\right)\hat{P}^{-1} = i\hbar\frac{\partial}{\partial t}; \qquad (12)$$

then $\hat{P}$ is called a DS operator and the TDSE will be said to possess this DS. When the TDSE with initial condition (I.C.) $\Psi|_{t=t_0}$ is operated by $\hat{P}$, the same equation of motion is obtained (unity is inserted where required):

$$\begin{aligned} i\hbar\frac{\partial}{\partial t}\Psi = \hat{H}\Psi, \quad \text{I.C.: } \Psi|_{t=t_0}\hat{P}\left(i\hbar\frac{\partial}{\partial t}\hat{P}^{-1}\hat{P}\Psi\right) \\ = \hat{P}(\hat{H}\hat{P}^{-1}\hat{P}\Psi), \quad \text{I.C.: } (\hat{P}\Psi)|_{t=t_0} i\hbar\frac{\partial}{\partial t}(\hat{P}\Psi) \\ = \hat{H}(\hat{P}\Psi), \quad \text{I.C.: } (\hat{P}\Psi)|_{t=t_0}. \end{aligned} \qquad (13)$$

Only the boundary conditions can distinguish between $\Psi$ and $(\hat{P}\Psi)$. If $\Psi|_{t=t_0}$ is invariant under $\hat{P}|_{t=t_0}$ up to a phase factor $e^{i\alpha}$, then $\Psi$ and $(\hat{P}\Psi)$ will represent the same state, up to the same phase factor:

$$\hat{P}\Psi = e^{i\alpha}\Psi. \qquad (14)$$

[7]It is usually not possible to determine the DSs directly from a Hamiltonian that is written, for example, in second quantization.

From this analysis, which is called DSA, the symmetry properties of the wave function which solve that TDSE, and then of physical observable which are of interest, could be revealed. In our case, we are interested in all symmetry properties of the HHG spectra obtained from the Hamiltonian given in Eq. (7), which involve $\phi$. To perform DSA we need to first identify all the DS operations that involve $\phi$. It will then become possible to get a clue about the symmetries that the system may possess and under which conditions. Therefore DSA may help design the appropriate physical conditions that will support the existence of the symmetries and the correct simulations that would reveal under which conditions these symmetries appear. Let us look at the Hamiltonian in Eq. (7) with a sine-square envelope:

$$H(x,\, t;\, \phi) = -\frac{1}{2}\frac{\partial^2}{\partial x^2} - 0.63\exp(-0.1424x^2) + \varepsilon_0 x \sin^2\left(\frac{\omega t}{2N}\right)[\cos(\omega t) + \cos(2\omega t + \phi)], \quad (15)$$

and consider the following DS operator:

$$\hat{P} = e^{\pi(\partial/\partial\phi)}e^{(\pi/\omega)(\partial/\partial t)}e^{i\pi x(\partial/\partial x)},$$

which will be *symbolically* written as

$$\hat{P} = \left\{\phi \rightarrow \phi + \pi;\, t \rightarrow t + \frac{\pi}{\omega};\, x \rightarrow -x\right\}. \quad \text{(IIb)}$$

The Hamiltonian is invariant under the operation of this DS operator [shift every parameter of the Hamiltonian according to (IIb)], provided that the pulse supports many optical cycles ($N$ is large):

$$\lim_{N\to\infty} \hat{P}\hat{H}(x,\, t;\, \phi)\hat{P}^{-1} = \hat{H}(x,\, t;\, \phi); \quad (16)$$

that is, the Hamiltonian possesses the DS given in Eq. (IIb).[8] Now, when the DS operator $\hat{P}$ acts on the TDSE from the left we get ($N$ is large from now on):

$$i\hbar\frac{\partial}{\partial t}\Psi(x,\, t;\, \phi) = \hat{H}(x,\, t;\, \phi)\Psi(x,\, t;\, \phi)$$

$$i\hbar\frac{\partial}{\partial t}\Psi\left(-x,\, t + \frac{\pi}{\omega};\, \phi + \pi\right) = \hat{H}(x,\, t;\, \phi)\Psi\left(-x,\, t + \frac{\pi}{\omega};\, \phi + \pi\right), \quad (17)$$

where the initial conditions are respectively given by

$$\text{I.C.: } \Psi(x,\, t = 0;\, \phi) = \varphi_0(x)$$

$$\text{I.C.: } \Psi\left(-x,\, t + \frac{\pi}{\omega} = \frac{\pi}{\omega};\, \phi + \pi\right) = \varphi_0(x),$$

and $t$ is the physical time (the two above TDSE are integrated between $t = 0$ and $t = T_p$); the two differential equations above are the same (same Hamiltonian) and have the same initial condition (wave function at $t = 0$) $\varphi_0(x)$[9] and should therefore have the same solution. We conclude that the two wave functions are identical:

$$\Psi(x,\, t;\, \phi) = \Psi\left(-x,\, t + \frac{\pi}{\omega};\, \phi + \pi\right). \quad (18)$$

The result should be understood as follows: If the wave function is treated as an abstract object that depends on the variables $x$, $t$ and on all parameters that are controllable in the experiment (here these are $\hbar$, $m$, $i$, $e$, $N$, $\phi$ . . .) then, in the space of all variables and parameters, the relation in Eq. (18) exists.[10] Practically, the result states that the wave function obtained from solution of the TDSE with some relative phase $\phi$ in the Hamiltonian and initial condition $\Psi(x, t = 0; \phi) = \varphi_0(x)$ equals the wave function obtained from solution of another TDSE with a relative phase $\phi + \pi$ in the Hamiltonian and middle condition $\Psi(x, t = \pi/\omega; \phi + \pi) = \varphi_0(x)$, but the coordinate needs to be reversed and the time needs to be shifted by $\pi/\omega$. This middle condition could be set in the middle of the propagation but we wish to set the initial condition in all simula-

[8]The Hamiltonian possesses the DS given in Eq. (IIb) with any envelope that fulfills $f(t + \pi/\omega) \cong f(t)$, that is, with a CW envelope $f(t) = 1$, or with the slow-switched envelope $f(t) = 1 - \exp(-at^2)$ where $a$ is a small enough number. It is also evident that envelopes for which $f(t + \pi/\omega) \neq f(t)$ prevent the Hamiltonian from possessing the above DS, and so do field-free potentials that do not have the symmetry $V_0(x) = V_0(-x)$.

[9]The initial condition taken in the above TDSE is the ground state of the field-free Hamiltonian $\varphi_0(x)$. It is a (symmetric) function of the coordinate $x$ only, and is therefore invariant under $\hat{P}$. Hence, this initial condition is preserved in the second TDSE, under the operation of $\hat{P}$.

[10]It can be checked that other symmetries that exist are, for example, $\Psi(x, t; \phi, e) = \Psi(x, t + \pi/\omega; \phi + \pi, -e)$, $\Psi(x, t; e) = \Psi(-x, t; -e)$, etc.

tions, and the same one always, so we wish to carry out the simulation with the phase $\phi + \pi$ with the initial condition $\Psi(x, t = 0; \phi + \pi) = \varphi_0(x)$. The question therefore arises as to which cases $\Psi(x, t = \pi/\omega; \phi + \pi) \approx \Psi(x, t = 0; \phi + \pi)$, or in which cases the initial state would not change even after propagation of half cycle. The answer is clear: Whenever $N$ is large, the perturbation is weak at early times and the result in Eq. (18) is correct. The result is correct in general for any adiabatically switched pulses, such as $f(t) = 1 - e^{-at^2}$, $a \ll 1$.

Using Eq. (18) it is easily seen that the expectation values of the dipole, acceleration, and the expression for the HHG power spectra obtained from simulations done with relative phase $\phi$ or $\phi + \pi$ in the Hamiltonian are simply related ($L$ is any large number that satisfies $\Psi(|x| > L/2, t = T_p; \phi) = 0$):

$$\begin{aligned} d(t; \phi) &\equiv \int_{-L/2}^{L/2} |\Psi(x, t; \phi)|^2 e x dx \\ &= \int_{-L/2}^{L/2} \left|\Psi\left(-x, t + \frac{\pi}{\omega}; \phi + \pi\right)\right|^2 e x dx \\ &= -\int_{-L/2}^{L/2} \left|\Psi\left(y, t + \frac{\pi}{\omega}; \phi + \pi\right)\right|^2 e y dy \\ &= -d\left(t + \frac{\pi}{\omega}; \phi + \pi\right), \end{aligned} \quad (19)$$

and also

$$\begin{aligned} a(t; \phi) &\equiv \frac{1}{m} \int_{-L/2}^{L/2} |\Psi(x, t; \phi)|^2 \left( - \frac{\partial V_0(x)}{\partial x} \right. \\ &\left. + e \cdot f(t) \cdot E(t, \phi) \right) dx = \frac{1}{m} \int_{-L/2}^{L/2} \left|\Psi\left(-x, t + \frac{\pi}{\omega}; \right.\right. \\ &\left.\left. \phi + \pi\right)\right|^2 \left( \frac{\partial V_0(-x)}{\partial(-x)} - e \cdot f\left(t + \frac{\pi}{\omega}\right) \cdot E\left(t + \frac{\pi}{\omega}, \right.\right. \\ &\left.\left. \phi + \pi\right)\right) dx = \frac{1}{m} \int_{-L/2}^{L/2} \left|\Psi\left(y, t + \frac{\pi}{\omega}; \phi + \pi\right)\right|^2 \left( \frac{\partial V_0(y)}{\partial(y)} \right. \\ &\left. - e \cdot f\left(t + \frac{\pi}{\omega}\right) \cdot E\left(t + \frac{\pi}{\omega}, \phi + \pi\right)\right) dy \\ &= -a\left(t + \frac{\pi}{\omega}; \phi + \pi\right), \end{aligned} \quad (20)$$

where the last result also follows immediately from Eq. (19) by taking the second time derivative of the dipole. So we get

$$\begin{aligned} \sigma(\Omega; \phi) &= \left| \frac{1}{T_p} \int_0^{T_p} a(t; \phi) e^{-i\Omega t} dt \right|^2 \\ &= \left| -\frac{1}{T_p} \int_0^{T_p} a\left(t + \frac{\pi}{\omega}; \phi + \pi\right) e^{-i\Omega t} dt \right|^2 \\ &= \left| -e^{i\Omega(\pi/\omega)} \frac{1}{T_p} \int_{0+\pi/\omega}^{T_p+\pi/\omega} a(\tau; \phi + \pi) e^{-i\Omega\tau} d\tau \right|^2 \\ &\approx \sigma(\Omega; \phi + \pi). \end{aligned} \quad (21)$$

We conclude that when the Hamiltonian in Eq. (15) is taken and the pulse is long, the HHG spectra obtained from simulation done with relative phase $\phi$ in the Hamiltonian equals the HHG spectra obtained from another simulation done with relative phase $\phi + \pi$ [where the initial condition for both simulations is $\Psi(x, t = 0; \phi) = \varphi_0(x)$]. We may generalize these conclusions and say they hold for every 1D model with symmetric field-free potential, symmetric initial condition, and adiabatically switched pulse.

The Hamiltonian in Eq. (15) is also invariant under the following second-order DS operation (it is easily seen that the square of this DS operator is just unity, hence the terminology "second order")

$$\hat{O}_2 = \{\phi \rightarrow -\phi; t \rightarrow NT - t; i \rightarrow -i\}. \quad \text{(Ib)}$$

The Hamiltonian possesses the DS given in Eq. (Ib) for any value of $N$:[11]

$$\hat{O}_2 \hat{H}(x, t; \phi) \hat{O}_2^{-1} = \hat{H}(x, t; \phi). \quad (22)$$

Now, when the DS operation $\hat{O}_2$ acts from the left on the TDSE we get:

$$\begin{aligned} i\hbar \frac{\partial}{\partial t} \Psi(x, t; \phi) &= \hat{H}(x, t; \phi) \Psi(x, t; \phi) \\ i\hbar \frac{\partial}{\partial t} \Psi^*(x, NT - t; -\phi) &= \hat{H}(x, t; \phi) \Psi^*(x, NT - t; -\phi), \end{aligned} \quad (23)$$

[11]The Hamiltonian possesses the DS given in Eq. (Ib) with any envelope that fulfills $f(NT - t) = f(t)$, that is, with any symmetric envelope, for example a trapezoid envelope.

where the initial conditions are transformed accordingly,

$$\text{I.C.: } \Psi(x, t = 0; \phi) = \varphi_0(x)$$

$$\text{I.C.: } \Psi^*(x, NT - t = NT; -\phi) = \varphi_0(x).$$

Because the Hamiltonians and the initial conditions of the two TDSE are the same, the two wave functions should be same. But are they the same? Does $\Psi(x, t; \phi)$ equal $\Psi^*(x, NT - t; -\phi)$? Apparently the wave function obtained from solution of the TDSE with some relative phase $\phi$ in the Hamiltonian and initial condition $\Psi(x, t = 0; \phi) = \varphi_0(x)$ should equal the complex conjugate of the wave function obtained from solution of another TDSE with a relative phase $-\phi$ in the Hamiltonian and final condition $\Psi^*(x, t = NT; -\phi) = \varphi_0(x)$, but the time needs to be reversed. However, the requirement $\Psi^*(x, t = NT; -\phi) = \varphi_0(x)$, which could also be written as $\Psi(x, t = NT; -\phi) = \varphi_0(x)$, is *usually* never fulfilled because the same initial conditions are used in all simulations. It is known that $\Psi(x, t = 0; -\phi) = \varphi_0(x)$, and there is no reason why in a system with open channels (ionization may occur) the wave function would remain the same at the end of propagation. Hence one should not expect that the wave function $\Psi(x, t; \phi)$ would equal $\Psi^*(x, t = NT; -\phi)$, and thus the HHG spectra obtained from simulations with phases $\phi$ and $-\phi$ is not the same. Only if an initial condition in the simulation with phase $-\phi$ is taken such that it yields at the end of the propagation a final wave function that equals $\varphi_0(x)$, then the two wave functions will be related by $\Psi(x, t; \phi) = \Psi^*(x, NT - t; -\phi)$ and the same HHG spectra will be obtained in both simulations. However, such a bizarre condition is not taken in our simulations:

$$\Psi(x, t; \phi) \neq \Psi^*(x, NT - t; -\phi) \tag{24}$$

$$\sigma(\Omega; \phi) \neq \sigma(\Omega; -\phi). \tag{25}$$

It should be noted that the fact that we cannot prove that $\Psi(x, t; \phi)$ equals $\Psi^*(x, NT - t; -\phi)$ does not provide a negative proof. A complete negative proof, i.e., $\Psi(x, t; \phi) \neq \Psi^*(x, t = NT; -\phi)$, cannot be based on the properties of a specific DS operator since one cannot be sure that hidden higher-order symmetries do not exist in the problem. In addition, even if it could be proven that $\Psi(x, t; \phi) \neq \Psi^*(x, t = NT; -\phi)$, it does not necessarily mean that the HHG spectra is different. The bottom line is that analysis based on DSs can only show the existence of equalities and not of inequalities.

It is clear that a nonsymmetric envelope of the laser pulse, for example, prevents the Hamiltonian from possessing the second DS. Other parameters that were also taken as symmetric functions in order not to prevent the Hamiltonian from possessing a possible DS are the shape of the field-free potential and the shape of the initial wave function.

Now that it is understood which kind of DSs may exist in the problem and which parameters may influence their existence, it is possible to design useful simulations that will demonstrate the existence of these symmetries in the system. But could these results be seen also in the laboratory, in a real experiment?

The DSA for time-dependent problems in 1D could easily be extended to the 3D case. Say we have a 3$Z$-dimensions atom of $Z$ electrons, denoted by the Hamiltonian

$$H(\mathbf{r_1}, \mathbf{r_2}, \ldots, \mathbf{r_Z}, t; \phi) = \sum_{i=1}^{Z} \frac{\mathbf{p}_i^2}{2m} - \sum_{i=1}^{Z} \frac{e}{|\mathbf{r_i}|} + \sum_{i<j} \frac{e}{|\mathbf{r_i} - \mathbf{r_j}|}$$

$$- \sum_{i=1}^{Z} e\mathbf{r_i} \cdot \mathbf{E_0} \sin^2\left(\frac{\omega t}{2N}\right)[\cos(\omega t) + \cos(2\omega t + \phi)], \tag{26}$$

where $\mathbf{r_i}$ are the different 3D electronic coordinates and we assume dipole approximation ($\mathbf{E_0}$ is not a function of the electron coordinates). By the exact same procedure as used in Eq. (17), it can be shown that if the initial wavefunction is symmetric $\Psi(\mathbf{r_1}, \mathbf{r_2}, \ldots \mathbf{r_Z}, t = 0; \phi) = \Psi(-\mathbf{r_1}, -\mathbf{r_2}, \ldots - \mathbf{r_Z}, t = 0; \phi)$ then it holds the following symmetry: $\Psi(\mathbf{r_1}, \mathbf{r_2}, \ldots \mathbf{r_Z}, t; \phi) = \Psi(-\mathbf{r_1}, -\mathbf{r_2}, \ldots - \mathbf{r_Z}, t + (\pi/\omega); \phi + \pi)$ and therefore the HHG spectra holds the symmetry $\sigma(\Omega; \phi) = \sigma(\Omega; \phi + \pi)$, provided that $N$, the number of oscillations the pulse supports, is large. The result is also correct for any adiabatically switched pulse.

In this section we have shown by carrying out the DSA that for the Hermitian Hamiltonian given in Eq. (7) with the *symmetric* initial condition $\varphi_0(x)$ and adiabatic sine-square laser pulse which supports $N$ optical cycles:

$$\sigma(\Omega; \phi) \neq \sigma(\Omega; -\phi)$$

$$\sigma(\Omega; \phi) = \sigma(\Omega; \phi + \pi) \tag{27}$$

or

$$\Delta\sigma_{\mathrm{I}}(\Omega) \neq 0$$

$$\lim_{N\to\infty} \Delta\sigma_{\mathrm{II}}(\Omega) = 0. \tag{28}$$

Why does $\Delta\sigma_{\mathrm{I}}(\Omega) \neq 0$ even in the case that the laser pulse supports infinite number of optical cycles, although we have proved before that $\Delta\sigma_{\mathrm{I}}(\Omega) = 0$ for a single Hermitian Floquet state? The answer is that within the conventional (Hermitian) QM only for bound systems (no ionization) the adiabatic laser pulse transfers a single bound eigenstate of the field-free Hamiltonian to a single Hermitian quasi-energy (QE) Floquet state. Therefore, for bound systems, a single Floquet state controls the photo-induced dynamics. However, in the case of open systems where ionization takes place, the QE spectrum is continuous and therefore the photo-induced dynamics is controlled by a wave packet that can be described as a linear combination of QE Floquet states that are discrete only due to the use of finite number of grid or finite number of basis functions in the numerical calculations. In such a case, we mix Hermitian Floquet QE states with different DS properties, which results in $\Delta\sigma_{\mathrm{I}}(\Omega) \neq 0$. Only within the framework of the NHQM is the photo-induced dynamics controlled by a single Floquet state (which is very different from the Floquet states obtained from the conventional QM calculations), even when ionization occurs [14].

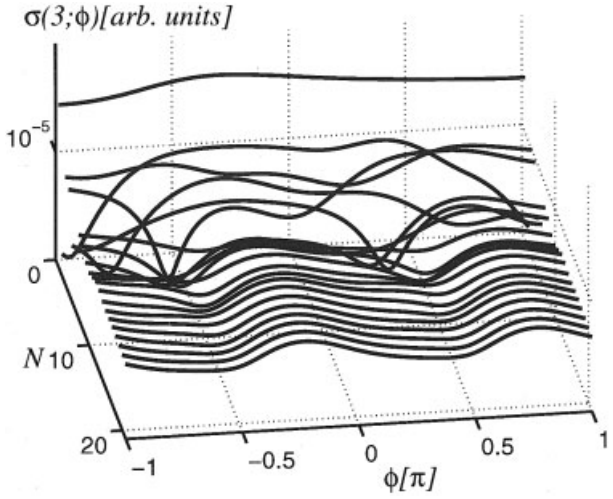


**FIGURE 3.** The third harmonic as function of $\phi$ and $N$ obtained from a Xe-atom simulation. It can be clearly seen that only the translational symmetry exists, and only if $N$ is large.

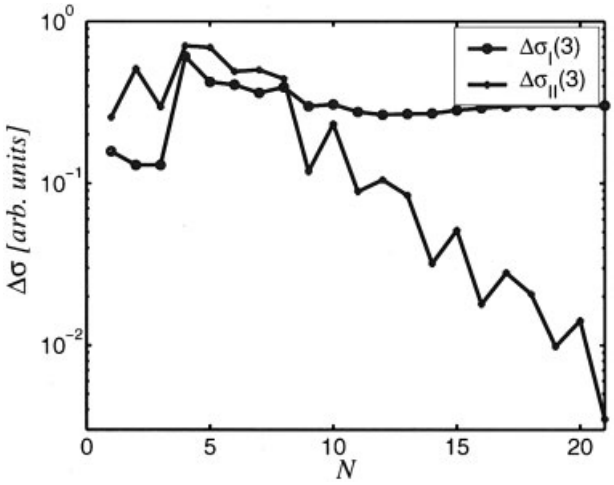


**FIGURE 4.** The asymmetry parameters as function of $N$ for the Xe-atom simulation. As the pulse becomes longer, only the translational symmetry reveals itself.

We conclude that the two parameters that influence the existence of symmetries (I) or (II) are the adiabaticity of the laser pulse and the existence of ionization in the model. Therefore these are the parameters we are going to check in numerical simulations. We also conclude that symmetry (I) exists when there is no ionization *and* the perturbation is close to be adiabatic. For symmetry (II) to exist it is sufficient that the perturbation is close to be adiabatic. Because we are studying a sine-square laser pulse, the adiabaticity criteria is represented by the length of the laser pulse.

## 4. Symmetry Properties of HHG Spectra as a Function of Duration of Sine-Square Laser Pulse

We study the interaction of a Xe atom with a sine-square laser pulse, which is described by the Hamiltonian given in Eq. (15). The TDSE is integrated with no additional approximations on a spatial grid using the Forest–Ruth split-operator algorithm. The grid size is taken large enough to avoid any reflections from its boundaries. The field-free potential possesses both bound states and continuum states (positive energy states) that represent ionizing channels, so ionization exists in the model. The results revealed in the numerical simulations, match the results predicted by DSA, as can be

shown in Figures 3 and 4. The only symmetry we expect is the symmetry with respect to translation of $\phi$, because ionization in the system will prevent the appearance of the other symmetry. Indeed, we see in Figure 4 that only the translational symmetry is obtained as the duration of the laser pulse increases; in Figure 3 we see that a pulse that supports as little as 14 oscillations is already considered as "adiabatic," since the translational symmetry pattern is recovered only for pulses longer than that.

To study the effect of photo-induced ionization on the symmetry properties of the HHG spectra, we solve another model Hamiltonian for the Xe atom in which ionization is not possible. We take a two-level Xe-atom model submitted to a sine-square laser pulse and use the sixth-order Runga–Kutta–Verner algorithm to solve the two coupled differential equations. The two lowest states of the field-free Xe-atom model are used as a basis set to describe the time dependent wave function:

$$\Psi(x, t; \phi) = c_0(t; \phi)\varphi_0(x) + c_1(t; \phi)\varphi_1(x), \quad \text{I.C.: } \Psi(x, t = 0; \phi) = \varphi_0(x), \tag{29}$$

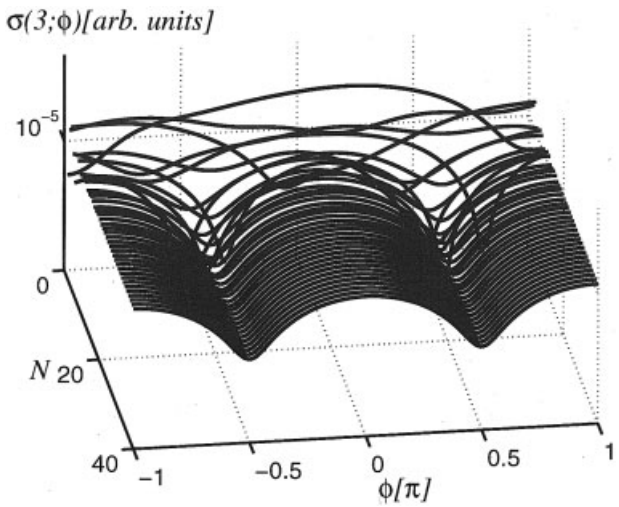


**FIGURE 5.** The third harmonic as function of $\phi$ and $N$, the number of optical cycles the pulse supports, obtained from a two-level Xe-atom simulation. It can be clearly seen that both symmetries involving $\phi$ exist. In this specific simulation the electric field used was 100 times stronger than in other simulations ($\varepsilon_0 = 3.5$ a.u.) in order for the symmetries to be pronounced in the spectrum.

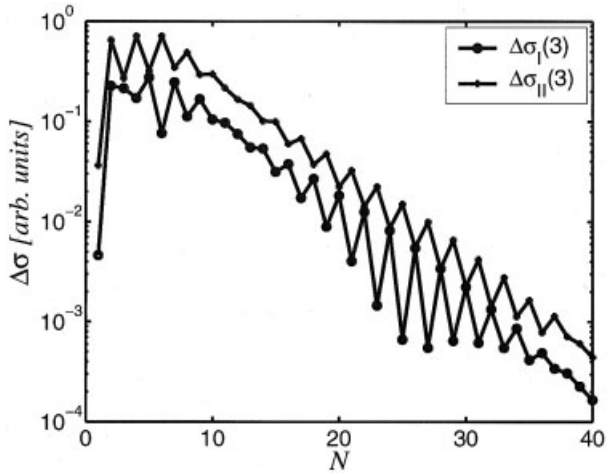


**FIGURE 6.** The asymmetry parameters as function of $N$, the number of optical cycles the pulse supports, for the two-level Xe-atom simulation. Both asymmetry parameters tend to zero as the pulse becomes longer, thus representing the appearance of both symmetries.

and the Hamiltonian of the system is that of Eq. (15). The evolution of the system is described by the TDSE

$$i\hbar \frac{\partial}{\partial t}\begin{bmatrix} c_0(t; \phi) \\ c_1(t; \phi) \end{bmatrix} = \begin{bmatrix} E_0 & \mu_{01}(t) \\ \mu_{01}(t) & E_1 \end{bmatrix} \cdot \begin{bmatrix} c_0(t; \phi) \\ c_1(t; \phi) \end{bmatrix}, \tag{30}$$

where

$$E_i = \left\langle \varphi_i(x) \middle| -\frac{\hbar^2}{2m}\frac{\partial^2}{\partial x^2} + V_0(x) \middle| \varphi_i(x) \right\rangle,$$

$$\mu_{ij} \equiv \sin^2\left(\frac{\omega t}{2N}\right) \cdot E(t, \phi) \cdot \langle \varphi_i(x)|x|\varphi_j(x)\rangle \quad i, j = 0, 1.$$

No ionization exists in the system, therefore we expect to get both symmetries as the pulse becomes longer. The results of the numerical simulations match our predictions, as shown in Figures 5 and 6. In Figure 6 we see that both symmetries are obtained as the pulse gets longer and from Figure 5 it is evident that a pulse supporting 20 oscillations or more is to be considered "long."

## 5. The Symmetry Properties of Intense-Field Ionization as Function of the Duration of the Sine-Square Laser Pulse

Intense field ionization of a single active electron in an atom has several distinct regimes [23, 24] that

depend on the combination of two parameters: the field's *intensity* and *frequency*. As the light intensity increases and/or its frequency decreases, the ionization mechanism may switch from multiphoton to above-threshold (ATI) tunneling and over-the-barrier ionization. When the laser field intensity is not very high (and the frequency is high), the ionization probability per cycle is very small; this is the regime of multiphoton ionization, which could be described in the frame of low-order perturbation theory and the rates of ionization are given by Fermi's golden rule. ATI takes place when the laser field becomes intense enough to make the ponderomotive energy of the ionized electron (approximately the averaged kinetic energy acquired by a free electron in the oscillating laser field) larger than the photon energy but not too high so the ionization probability per cycle remains small. Because it is difficult to describe ATI in the frame of even high-order perturbation theory, nonperturbative methods should be applied. The ionization rate is still a well-defined function of the intensity.

Tunneling occurs at higher field intensities (small frequencies) when ionization probability per cycle becomes significant. In this regime, the tunneling ionization rate no longer depends on intensity but on the instantaneous electric field amplitude, which it completely traces. In the quasi-state *dc* limit the rate $w(t; \phi)$ is an exponential function of the instantaneous field amplitude [25–27], as seen in Eq. (31). The probability to ionize is obtained by integration of this rate:

$$w(t;\,\phi) = 4(2I_p^{5/2})\,\frac{1}{E(t;\,\phi)}\exp\left[-\frac{2}{3}(2I_p^{3/2})\,\frac{1}{E(t;\,\phi)}\right] \tag{31}$$

$$P_{\text{ion}}^{\text{tun}}(t;\,\phi) = \int_0^t w(t';\,\phi)dt'. \tag{32}$$

If the field intensity is so high as to completely deplete the bound state on a single cycle, the ionization is said to be in the over-the-barrier regime. It should be emphasized that both intensity and frequency of the electric field determine the type of ionization; at very high frequencies of the field (and almost regardless of its intensity) the electron may cease to react to the field. In this regime, which is called the stabilization regime, ionization is suppressed.

In our simulation ionization occurs on the border between ATI and tunneling. This is revealed from the Keldysh parameter, which is a dimensionless parameter that characterizes, by its different values, the different ionization regimes

$$\gamma = \sqrt{\frac{I_p}{2U_p}} \tag{33}$$

where $I_p$ is the field-free ionization potential and $U_p$ is the ponderomotive energy, which for the bichromatic case with one frequency the second harmonic of the other and equal single-frequency intensities is

$$U_p = \frac{e^2\varepsilon_0^2}{4m}\left(\frac{1}{\omega^2} + \frac{1}{(2\omega)^2}\right). \tag{34}$$

The Keldysh parameter can be thought of as the time it takes an electron to tunnel through the atom–laser potential barrier in units of the optical period. Ionization is expected to be dominated by ATI when $\gamma \gg 1$ and by tunneling when $\gamma \ll 1$. In our simulation, the intense-field ionization occurs under conditions such that $\gamma \approx 2$, far from the tunneling or the ATI regime. Nevertheless, as will be shown, the ionization probability has a strong phase dependence, thus implying that the ionization occurs near the tunneling regime.

Because the tunneling potential oscillates back and forth with the laser field, ionization may occur in two directions along the laser polarization. We calculate the probability to ionize to the left and to the right. Their sum is the total probability to ionize. The electronic density released to the continuum, when a 10-oscillations pulse with relative phase $\phi = 0.625\pi$ is switched on is plotted in Figure 7 as a function of both coordinate and time. The shape of the laser field is also plotted, beneath the density, on a much larger scale in order to fit the plot. The density released to the continuum is the modulus square of $|\Psi_{\text{ion}}(x, t; \phi)\rangle$, the projection of the wave function on the continuum states which equals also the total wave function from which the projection on the three bound states of the potential $V_0(x)$ (Fig. 1) has been subtracted:

$$|\Psi_{\text{ion}}(x, t; \phi)\rangle = |\Psi(x, t; \phi)\rangle - \sum_{i=0}^{2}\langle\varphi_i(x)|\Psi(x, t; \phi)\rangle|\varphi_i(x)\rangle. \tag{35}$$

As one sees, as time passes, the amount of density released into the continuum (the probability to

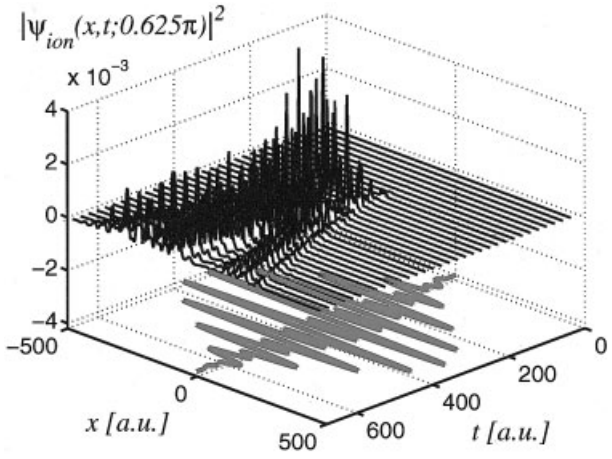


**FIGURE 7.** The time and coordinate dependence of the continuum-released density, which results from the action of a 10-oscillation pulse with $\phi = 0.625\pi$ on the Xe atom. The time-dependent electric field is plotted on the surface formed by the two independent axes, $x$ and $t$, with the positive direction of the coordinate as the positive direction of the field. As time passes, the amount of density released into the continuum increases, but reaches a final value, as the pulse ends.

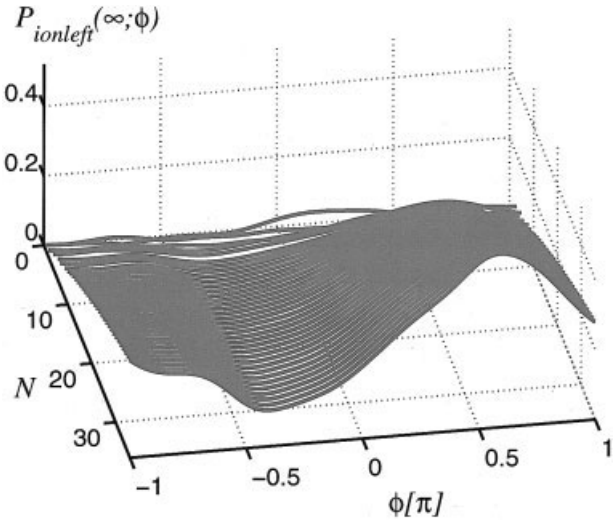


**FIGURE 8.** The final probability to ionize to the left, as function of $\phi$ and $N$, obtained from a Xe-atom simulation. As $N$ gets bigger, the probability increases. A cut made in the $P$–$N$ plane (for any value of $\phi$) would show that the ionization probability approaches unity, as $N$ goes to infinity.

ionize) increases and reaches a steady value as the laser pulse ends. Integration of this density over the coordinate at that time, or at any other later time, gives the final probability of the atom to ionize, which will be denoted as $P_{\text{ion}}(\infty;\ \phi)$, where the time-dependent probability to ionize is given by

$$P_{\text{ion}}(t;\ \phi) = \langle \Psi_{\text{ion}}(x,\ t;\ \phi) | \Psi_{\text{ion}}(x,\ t;\ \phi) \rangle. \qquad (36)$$

We shall also define the probability to ionize "to the left" (the probability to ionize to the direction of $-x$), which is obtained by integration of the continuum density in the interval $[-\infty,\ 0]$, and the probability to ionize "to the right" (as the probability to ionize to the direction of $+x$):

$$P_{\text{ionleft}}(t;\ \phi) = \int_{-\infty}^{0} |\Psi_{\text{ion}}(x,\ t;\ \phi)|^2 dx \qquad (37)$$

$$P_{\text{ionright}}(t;\ \phi) = \int_{0}^{\infty} |\Psi_{\text{ion}}(x,\ t;\ \phi)|^2 dx. \qquad (38)$$

Figure 7 shows that for this specific value of $\phi$, the probability to ionize to the left is greater than the probability to ionize to the right. We can do this type of simulation for different values of the phase $\phi$ and reveal the symmetry properties of the directional (left-right) and total ionization probabilities. As seen in Figures 8–10, the probabilities to ionize

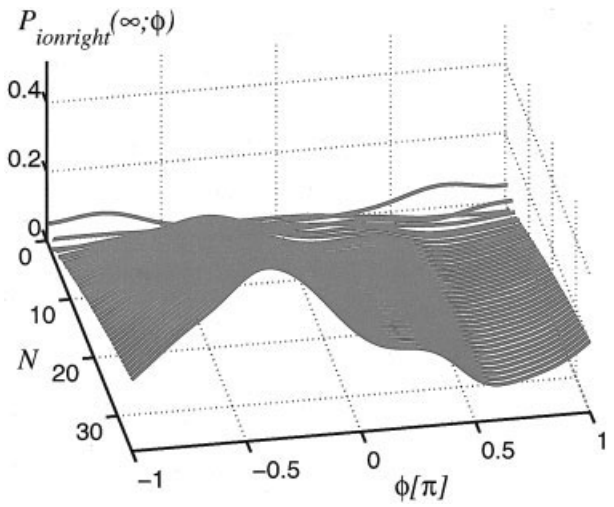


**FIGURE 9.** The final probability to ionize to the right, as function of $\phi$ and $N$, obtained from a Xe-atom simulation. As $N$ gets bigger, the $\phi$-dependence of the right-ionization probability and of the left-ionization probability becomes the same, up to a shift by $\pi$ (compare with Fig. 8).

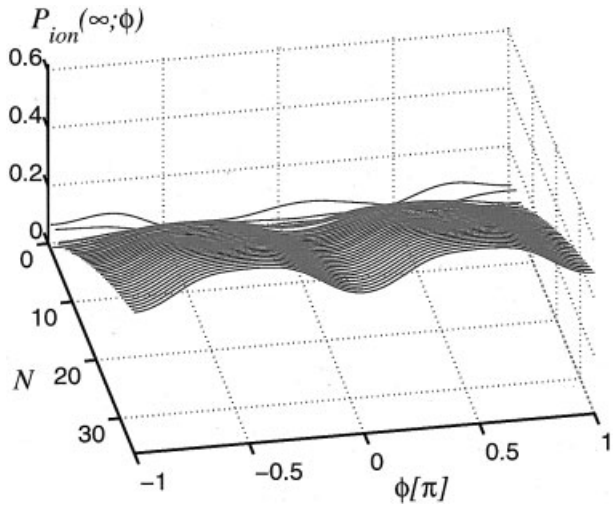


**FIGURE 10.** The final total probability to ionize as function of $\phi$ and $N$, obtained from a Xe-atom simulation. As $N$ gets bigger, the probability shows both symmetries [Eqs. (43), (44)].

to the left, to the right, or the total probability to ionize are all functions that strongly depend on the relative phase $\phi$. Different values of $\phi$ induce different amounts of ionizations. This is a well-known phenomenon, and was shown already in the referenced works.

It is evident from the figures that, at long laser pulses, the final probabilities to ionize to the left and to the right are the same function of $\phi$, up to a shift by $\pi$. These results are obvious. We obtained before that when two simulations are done with phases $\phi$ and $\phi + \pi$, with the same initial condition $\varphi_0(x)$, according to the Hamiltonian given in Eq. (15) with a sine-square pulse, then for long laser pulses the wave functions of the two simulations are related as seen in Eq. (18); therefore the same connection should hold also for $|\Psi_{\text{ion}}(x,\ t;\ \phi)\rangle$. We can use the symmetry properties of the three bound states of the field-free Hamiltonian[12] and show it:

$$\Psi_{\text{ion}}(x,t;\phi) = \Psi(x,t;\phi) - \sum_{i=0}^{2}\varphi_i(x)\int_{-L/2}^{L/2}\varphi_i(x')\Psi(x',t;\phi)dx' = \Psi\left(-x,t+\frac{\pi}{\omega};\phi+\pi\right)$$
$$-\sum_{i=0}^{2}\varphi_i(x)\int_{-L/2}^{L/2}\varphi_i(x')\Psi\left(-x',t+\frac{\pi}{\omega};\phi+\pi\right)dx' = \Psi\left(-x,t+\frac{\pi}{\omega};\phi+\pi\right) - \sum_{i=0}^{2}\varphi_i(-x)\int_{-L/2}^{L/2}$$
$$\times\ \varphi_i(-x')\Psi\left(-x',t+\frac{\pi}{\omega};\phi+\pi\right)dx' = \Psi\left(-x,t+\frac{\pi}{\omega};\phi+\pi\right) - \sum_{i=0}^{2}\varphi_i(-x)\int_{-L/2}^{L/2}$$
$$\times\ \varphi_i(y)\Psi\left(y,t+\frac{\pi}{\omega};\phi+\pi\right)dy = \Psi_{\text{ion}}\left(-x,t+\frac{\pi}{\omega};\phi+\pi\right) \quad (39)$$

and using Eqs. (18) and (36) it can be easily shown that the total probability to ionize is the same (up to a time shift):

$$P_{\text{ion}}(t;\phi) = P_{\text{ion}}\left(t+\frac{\pi}{\omega};\phi+\pi\right). \quad (40)$$

The properties that depend on direction, however, such as the directional probabilities to ionize, are inverted because the coordinate also needs to be inverted in comparing the two simulations. Using Eqs. (18) and (37)–(38) we easily get:

$$P_{\text{ionleft}}(t;\phi) = P_{\text{ionright}}\left(t+\frac{\pi}{\omega};\phi+\pi\right) \quad (41)$$

$$P_{\text{ionright}}(t;\phi) = P_{\text{ionleft}}\left(t+\frac{\pi}{\omega};\phi+\pi\right). \quad (42)$$

This means that the probability to ionize to the right ($+x$) in the first simulation equals the probability to ionize to the left ($-x$) in the second simulation, up to a time shift. Hence, for long laser pulses, the final probabilities to ionize to the left and to the right are the same function of $\phi$, up to a shift by $\pi$, as can be easily seen in the results. The final ionization probability is calculated from the final (field off) electronic density released into the continuum, at some time ($t \geq T_p$) where this density

[12] $\varphi_0(x) = \varphi_0(-x)$, $\varphi_1(x) = -\varphi_1(-x)$ and $\varphi_2(x) = \varphi_2(-x)$. Therefore, for every bound state, $\varphi_i(x)\varphi_i(x') = \varphi_i(-x)\varphi_i(-x')$.

has already reached a steady value and is not a function of time anymore. Hence additional propagation by $\pi/\omega$ would not influence the final ionization probability and the final conclusion.

Provided that the laser pulse is long enough, the final total probability to ionize is symmetric both to inversion in $\phi$ and translation by an angle of $\pi$, as seen in Figure 10. The origin of the second symmetry is in the properties of the right-ionization and left-ionization functions:

$$P_{\text{ion}}(\infty; \phi) = P_{\text{ion}}(\infty; -\phi) \tag{43}$$

$$P_{\text{ion}}(\infty; \phi) = P_{\text{ion}}(\infty; \phi + \pi). \tag{44}$$

The strong phase dependence of the ionization probability implies that the ionization has some tunneling character. However, tunneling is not the only mechanism through which ionization takes place in our simulations, since our results differ from those predicted by the tunneling model in Eq. (32) (Fig. 11).

We would like also to refer to the results obtained in Ref. [14], where a complex-scaled Floquet Hamiltonian was used to describe the dynamics of the system subjected to a CW perturbation. From that simulation, values of the most long-living resonance quasi-energy lifetime (the decay rate) as a function of $\phi$ could be obtained. These values of lifetimes are symmetric both to inversion in $\phi$ and translation by an angle of $\pi$. These values could also be obtained from time-dependent simulation where an electric field is slowly switched on until it reaches a steady value on which it remains constant, representing thus an adiabatically switched CW perturbation ($1 - \exp(-at^2)$ $a \ll 1$, for example). If the time-dependent ionization probability obtained with some value of $\phi$ is plotted as function of time, we see an exponential-like curve that approaches asymptotically to unity, and the rising constant of this curve is the decay rate $\Gamma$ (see Fig. 12). The adiabatic process assures that only a single resonance Floquet state is populated and therefore the curve has a *single* raising constant. The values of $\Gamma$ obtained here and the values of the most long-living resonance quasi-energy lifetime obtained from the non-Hermitian simulation match, as shown in Figure 13. This result is a demonstration of the power and accuracy that time-independent non-Hermitian simulations have over the usual time-consuming time-dependent Hermitian simulations.

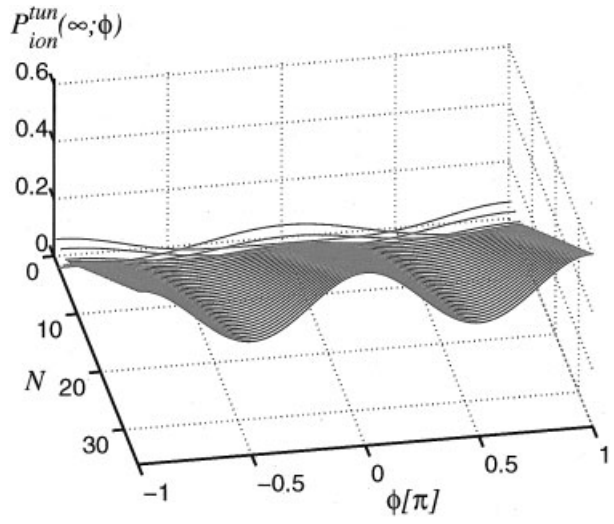


**FIGURE 11.** The final total probability to ionize as function of $\phi$ and $N$, obtained from the tunneling model [Eq. (32)]. As $N$ gets bigger, the probability shows both possible symmetries but is opposite to the probability that we got (Fig. 10).

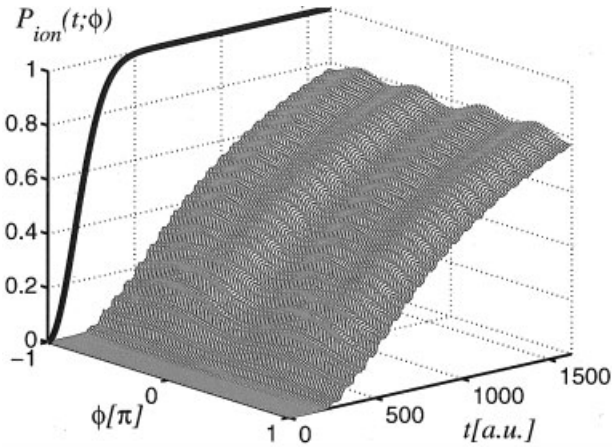


**FIGURE 12.** The total probability to ionize as function of time and $\phi$, obtained from simulation of a Xe atom subjected to an adiabatically switched 24-oscillation pulse with envelope $f(t) = 1 - \exp(-at^2)$, $a = 2 \cdot 10^{-5}$ (which is plotted on the $P$–$t$ plane). A cut done in the $P$–$t$ plane, for every value of $\phi$, will show that the time-dependent ionization probability approaches to unity exponentially, at least at late enough times, after the incubation period of the system, and the rising constant equals the decay rate of the system $\Gamma$. Different values of $\phi$ will produce different values of $\Gamma$, shown in Figure 13 as crosses.

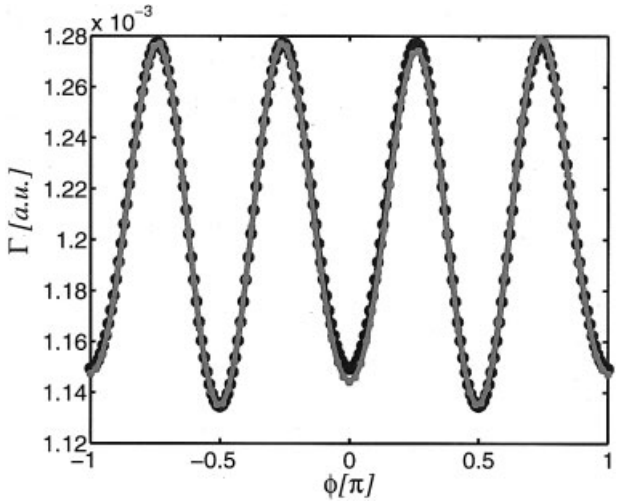


**FIGURE 13.** The width (decay rate) of the long-living resonance as a function of $\phi$ obtained from a non-Hermitian Floquet simulation (cycles) and decay rates obtained from the ionization probabilities of a Xe atom subjected to an adiabatically switched pulse, as a function of $\phi$ (crosses). The perfect match between the values obtained from the usual time-dependent propagation and the non-Hermitian stationary treatment reflects the equivalence of the two methods.

## 6. Conclusions

The phase dependence of HHG and intense-field ionization probability in an 1D Xe atom with symmetric field-free potential and symmetric initial wavefunction were studied numerically and analytically. From simulations based on a single-particle response it can be seen that the HHG spectra is symmetric with respect to inversion in the relative phase between the two colors $\phi$ only if ionization is forbidden in the system and the laser pulse is adiabatic. The HHG spectra is symmetric with respect to a $\pi$-shift in $\phi$ whenever the laser pulse is adiabatic. At the limit of an extremely adiabatic pulse, the system could be treated as subjected to a CW laser and could be analyzed within the framework of Floquet theory. Indeed, the results based on Floquet DSA, as was done in Ref. [14], agree with the results obtained here. Real physical systems usually may ionize and so, in experiments, a breaking of the first symmetry should occur.

If, in addition, experiments are done with short enough pulses (fs pulses), a breaking of the second symmetry should occur as well as enhanced breaking of the first symmetry. Fields of the form in Eq. (6) with parameters that make the dynamics belong to the tunneling regime can lead to very asymmetric ionization processes, ejecting electrons in the forward or backward direction preferentially, depending on the relative phase $\phi$, since this phase changes the instantaneous values of the time-varying electric field. The ionization probability is symmetric both to inversion or $\pi$-shift in $\phi$. The component probabilities (right- and left-ionization probabilities) have the same $\phi$-dependence, up to a shift of $\pi$. We hope that our results will stimulate experiments that explore the effect of the duration of the two-color laser pulse on the symmetry properties of the photo-induced ionization and the HHG spectra.

## References

1. Svanberg, S.; L'Huillier, A.; Wahlström, C. G. Nucl Instrum Methods Phys Res, Sect A 1997, 398, 55.
2. Kulander, K.; Schafer, K.; Krause, J. In Super-Intense Laser-Atom Physics; Piraux, B.; L'Huillier, A.; Rzążewski, K., Eds.; NATO Advanced Study Institutes, Series B: Physics, Vol. 316; Plenum Press: New York, 1993; p 95.
3. Lewenstein, M.; Balcou, P.; Ivanov, M. Y.; Corkum, P. B. Phys Rev A 1993, 49, 2117.
4. Salières, P.; L'Huillier, A.; Antoine, P.; Lewenstein, M. Adv At Mol Opt Phys 1999, 4, 83.
5. Alon, O. E.; Averbukh, V.; Moiseyev, N. Phys Rev Lett 1998, 80, 3743.
6. Ždánská, P.; Averbukh, V.; Moiseyev, N. J Chem Phys 2003, 118, 8726.
7. Gupta, A. K.; Moiseyev, N. Phys Rev B, submitted.
8. Alon, O. E.; Averbukh, V.; Moiseyev, N. Phys Rev Lett 2000, 85, 5218.
9. Long, S.; Becker, W.; McIver, J. K. Phys Rev A 1995, 52, 2262.
10. Figueira de Morisson Faria, C.; Milošević, D. B.; Paulus, G. G. Phys Rev A 2000, 61, 063415-1.
11. Bivona, S.; Burlon, R.; Leone, C. J Opt Soc Am 1999, 16, 986.
12. Schafer, K. J.; Kulander, K. C. Phys Rev A 1992, 45, 8026; Alon, O. E.; Moiseyev, N. Chem Phys 1995, 196, 499; Schumacher, D. W.; Weihe, F.; Muller, H. G.; Bucksbaum, P. H. Phys Rev Lett 1994, 73, 1344; Corkum, P. B. Phys Rev Lett 1993, 71, 1994.
13. Andiel, U.; Tsakiris, G. D.; Cormier, E.; Witte, K. Europhys Lett 1999, 47, 42.
14. Fleischer, A.; Averbukh, V.; Moiseyev, N. Phys Rev A 2004, 69, 043404/1.
15. Baltuska, A. Nature 2003, 421, 611.
16. Drescher, M.; Hentschel, M.; Kienberger, R.; Tempea, G.; Spielmann, C.; Reider, G.A.; Corkum, P. B.; Krausz, F. Science 2001, 291(5510), 1923.
17. Bandrauk, A.; Szczepan, C.; Hong, S. N. Phys Rev Lett 2002, 89, 283903.

18. Landau, L. D.; Lifshitz, E. M. Classical Theory of Fields, 4th ed.; Butterworth–Heinenann Press: Oxford, 1975.
19. Fleck, J. A.; Morris, J. R.; Feit, M. D. Appl Phys 1976, 10, 129; Feit, M. D.; Fleck, J. A.; Steiger, A. J Comput Phys 1982, 47, 412.
20. Forest, E.; Ruth, R. D. Physica D 1990, 43, 105; Campostrini, M.; Rossy, P. Nucl Phys B 1990, 329, 753; Candy, J.; Rozmus, W. J Comput Phys 1991, 92, 230.
21. Verner, J. H. SIAM J Numer Anal 1978, 15/4, 722; 1990, 27/5, 1332; 1991, 28/2, 496.
22. Levine, R. D. J Phys Chem 1985, 89, 2122.
23. Keldysh, L. D. Sov Phys JETP 1965, 20, 1307.
24. Delone, N. B.; Krainov, V. P. In Atoms in Strong Light Field; Springer: Berlin, 1985.
25. Landau, L. D.; Lifshitz, E. M. Quantum Mechanics; Pergamon: London, 1978.
26. Corkum, P. B.; Burnett, N. H.; Brunel, F. B. Phys Rev Lett 1989, 62, 1259.
27. Corkum, P. B.; Burnett, N. H.; Brunel, F. B. In Atoms in Intense Laser Fields, Gavrila, M., Ed.; Academic Press: Boston, 1992.